Journal of Nuclear Materials 397 (2010) 92–100

Contents lists available at ScienceDirect

Journal of Nuclear Materials

journal homepage: www.elsevier.com/locate/jnucmat

Aerosol behavior during SIC control rod failure in QUENCH-13 test

Terttaliisa Lind [a,*], Anna Pintér Csordás [b], Imre Nagy [b], Juri Stuckert [c]

[a] Paul Scherrer Institut, Villigen, Switzerland
[b] HAS KFKI Atomic Energy Research Institute, Budapest, Hungary
[c] Forschungszentrum Karlsruhe, Karlsruhe, Germany[1]

ARTICLE INFO

Article history:
Received 4 February 2009
Accepted 18 December 2009

ABSTRACT

In a nuclear reactor severe accident, radioactive fission products as well as structural materials are released from the core by evaporation, and the released gases form particles by nucleation and condensation. In addition, aerosol particles may be generated by droplet formation and fragmentation of the core. In pressurized water reactors (PWR), a commonly used control rod material is silver–indium–cadmium (SIC) covered with stainless steel cladding. The control rod elements, Cd, In and Ag, have relatively low melting temperatures, and especially Cd has also a very low boiling point. Control rods are likely to fail early on in the accident due to melting of the stainless steel cladding which can be accelerated by eutectic interaction between stainless steel and the surrounding Zircaloy guide tube. The release of the control rod materials would follow the cladding failure thus affecting aerosol source term as well as fuel rod degradation.

The QUENCH experimental program at Forschungszentrum Karlsruhe investigates phenomena associated with reflood of a degrading core under postulated severe accident conditions. QUENCH-13 test was the first in this program to include a silver–indium–cadmium control rod of prototypic PWR design. To characterize the extent of aerosol release during the control rod failure, aerosol particle size distribution and concentration measurements in the off-gas pipe of the QUENCH facility were carried out. For the first time, it was possible to determine on-line the aerosol concentration and size distribution released from the core. These results are of prime importance for model development for the proper calculation of the source term resulting from control rod failure.

The on-line measurement showed that the main aerosol release started at the bundle temperature maximum of $T \sim 1570$ K at hottest bundle elevation. A very large burst of aerosols was detected 660 s later at the bundle temperature maximum of $T \sim 1650$ K, followed by a relatively steady aerosol release until core cooling by quench when the on-line measurements were stopped. Cd was released first from the control rod, followed by In, and finally, by Ag. The particle size distributions were bimodal indicating two aerosol formation mechanisms, evaporation followed by nucleation and condensation, as well as droplet and fragment generation. Generally, release is modelled as evaporation from molten regions of control rod materials. Clearly, results of this investigation give evidence of contribution by entrainment of droplets and fragmented material.

1. Introduction

In a nuclear reactor severe accident, cooling of the core is lost and consequently, the core heats up to high temperatures. Chemical interactions between core materials induce fuel liquefaction and the fuel elements lose their integrity. Radioactive fission products as well as control rod and structural materials are released from the core by evaporation, and the released gases form particles by nucleation and condensation. In addition to aerosol formation by the gas-to-particle route, aerosol particles may also be generated by droplet formation and fragmentation of the core. In pressurized water reactors (PWR), a commonly used control rod material is silver–indium–cadmium (SIC) covered with stainless steel cladding. The control rod elements, Cd, In and Ag, have relatively low melting temperatures, and especially Cd has also a very low boiling point. Control rods are likely to fail early during the accident due to melting of the stainless steel cladding which can be accelerated by eutectic interaction between stainless steel and the surrounding Zircaloy guide tube. The release of the control rod materials would follow the cladding failure [1,2]. As release from the control rods can represent a large fraction of the total aerosol mass released, and as the released compounds may react with radiologically important iodine,

* Corresponding author. Tel.: +41 563102650.
E-mail address: terttaliisa.lind@psi.ch (T. Lind).
[1] Present name: Karlsruhe Institute of Technology.

0022-3115/$ - see front matter © 2009 Elsevier B.V. All rights reserved.
doi:10.1016/j.jnucmat.2009.12.013

the effect of the control rod failure is significant to the aerosol source term. In addition, control rod behavior has an influence on the fuel rod degradation.

The phenomena of control rod failure have been reviewed by Haste and Plumecocq [3]. First, Ag–In–Cd alloy melts at temperatures around 1050 K. When the pressure outside of the control rod is low, the stainless steel cladding may balloon due to the high pressure created by He or air inside the cladding, and Cd vaporization. The ballooning may cause contact between the stainless steel and the guide tube made of Zircaloy. This contact results in interaction of stainless steel and Zircaloy forming a low melting temperature eutectic, and consequently, breach in the control rod cladding. Often, the initial breach is small. At this point, Cd that is already in the vapor phase inside the control rod, is released through the breach, possibly along with droplets of molten material. Large failure of the control rod happens latest at the stainless steel melting temperature ~1690 K, releasing molten material that flows inside the core mainly downwards, along with vapors that form aerosol particles when the gas cools down. Evaporation of the control rod materials continues now from the molten material surface. The control rod failure mechanisms have been investigated in numerous single-effect tests [4] as well as more integral experiments, e.g. bundle tests CORA [5] and Phébus [6]. An overview of results of these and other integral tests on melt progression and corresponding final aerosol production was recently published [7]. However, time-dependent data on aerosol release from control rod rupture from realistic geometry are still missing, along with size distribution and composition data for the formed aerosol particles.

The QUENCH experimental program at Forschungszentrum Karlsruhe (FZK) investigates phenomena associated with reflood of a degrading core under postulated severe accident conditions, but where the geometry is still mainly rod-like and degradation is still at an early phase [8]. The experiment QUENCH-13 was the first in this programme to include a control rod of prototypic PWR design consisting of a SIC cylinder enclosed by stainless steel cladding within a Zircaloy guide tube [9–14]. The effects of the control rod on degradation and reflood behavior were examined under integral conditions, and for the first time the release of SIC aerosols following control rod rupture was measured. In particular, the expected sharp release of cadmium on control rod failure as well as the size of the generated particles were previously ill-defined experimentally. To characterize the extent of aerosol release during the control rod failure, aerosol particle size distribution and concentration measurements in the off-gas pipe of the QUENCH facility were carried out. For the first time, it was possible to determine on-line the aerosol concentration released from the control rod, as well as the size distribution of the aerosols. This along with analyses of the aerosol particle composition enabled us to determine the formation mechanisms of the aerosols formed during control rod failure.

2. Methods

2.1. QUENCH-13 test conduct

The QUENCH-13 test was performed at the Forschungszentrum Karlsruhe on 7 November 2007. The aim of the test was to investigate the effect of a SIC control rod on early-phase bundle degradation, and to measure release of SIC aerosols following control rod rupture in realistic geometry. The facility schematic and the cross-section showing the control rod in the middle of the electrically heated bundle are shown in Figs. 1 and 2. The test sequence involved pre-oxidation at temperatures below the minimum likely for control rod rupture, 1250 K, then a slow temperature increase to examine the rod rupture and aerosol release, and at last, quench water injection at the bottom of the test section, Fig. 3. The temperature increase was interrupted at approximately 11,600 s for 1000 s at the bundle temperature maximum of ~1630 K. Fig. 4 shows the hottest temperatures for the bundle ("Corner rod 950 mm") and the control rod ("Ag–In–Cd 950 mm"). The hottest elevation in the QUENCH bundle was at 950 mm. As the thermocouples in the control rod at this elevation and at elevation 850 mm were short-circuited at about 10,000 s by relocated melt, the thermocouple at 750 mm gives a good indication of the control rod temperature history.

2.2. Aerosol measurement set-up

The aerosols were sampled from QUENCH facility off-gas pipe at two locations with a gas temperature of about 570 K and a pressure of 2.0 bar(abs). Two sampling ports were located approximately 50 cm apart. The first aerosol port was used for continuous on-line measurements of aerosol particle size and concentration using electrical low-pressure impactor (ELPI) [15], and sequential measurements of aerosol particle size and mass concentration with Berner low-pressure impactors (BLPI) [16]. These measurements were carried out to determine the aerosol release from the SIC control rod, and the sampling system was isolated from the facility before core cooling by quench.

The second aerosol sampling port was used for an impactor system with 10 impactors (AEKI impactor), each of them operated for 1 min during the test. This system was used also during the quench phase of the test. In addition to sampling devices outside of the off-gas pipe, aerosols were collected during the whole experiment on a Ni plate that was placed inside the off-gas pipe under the ELPI–BLPI sampling nozzle [17–19].

Sampling nozzles in both aerosol sampling ports were elbow-type nozzles with an inner diameter of 10 mm. For on-line measurements, the sampling nozzle was connected to a ball-valve and then to a pre-cutter cyclone, Fig. 5. A three-stage ejector dilution system was mounted downstream of the cyclone. In the dilution system, three dilution units (Palas VKL-10) [20] were connected in series giving a total dilution ratio of 1:1600. The sample flow rate through the nozzle was 4.9 nlpm (normal liters/min). The sampling line from the off-gas pipe to the dilution system including the valve and the cyclone, as well as the first two dilution stages were heated up to 160–170 °C. In each dilution stage, 60 nlpm of clean, dry nitrogen was used as dilution gas. The dilution gas in the first dilution unit was heated up to 160 °C.

Particle size and concentration were measured on-line with an electrical low-pressure impactor (ELPI) which size-classifies particles according to their aerodynamic mobility into 12 size classes, or stages, in the particle size range D_{ae} = 0.03–10 μm. Here D_{ae} is the aerodynamic diameter of the particles, i.e., the size of a spherical particle of density 1.0 g/cm^3 and having the same aerodynamic mobility as the particle. The particles entering the device are charged in a corona charger to a known equilibrium charge distribution, and the current caused by the depositing particles on consecutive stages is measured with sensitive electrometers. Current on each stage is converted to particle number concentration. The number concentration was converted to mass concentration using a particle density of 10 g/cm^3 and assuming spherical particles. In the QUENCH-13 test, the flow into the ELPI was taken from the third stage of the three-stage dilution system resulting in the dilution ratio of 1:1600 for ELPI sample. The pressure was reduced to atmospheric pressure upstream of the ELPI in a critical orifice with diameter of 0.7 mm. Particle losses in the critical orifice were estimated to be small for particles smaller than approximately 3 μm which was the size range of main interest in this test. The losses may have been significant for larger particles. Further experimental work would be needed to accurately determine the contribution

of coarse particles (larger than approximately D_{ae} = 3 μm) for Ag, In and Cd release from the control rod.

The samples for size distribution and concentration determination with BLPI were taken downstream of the second dilution stage resulting in dilution ratio of 1:144. BLPI was heated up to 110 °C to avoid water condensation during sampling. In total, three samples were collected with BLPI during the test. The first sample BLPI1 was taken before control rod failure as a background sample, and two samples were taken after the control rod failure (Table 1). The mass size distribution was determined by weighing the BLPI substrates.

The 10-impactor system (AEKI impactor) was connected to the off-gas pipe without dilution, Fig. 6. The impactors had two collection stages, and a final quartz fiber filter which collected the smallest particle fraction, Fig. 7. The collector plate, which is first in the way of the gas stream, separates particles larger than D_{ae} = 5 μm; the next collector, which is near to the quartz fiber filter, collects particles with aerodynamic diameters between 1 and 5 μm. The quartz fiber filters collected mainly particles below D_{ae} = 1 μm. The impactor valves were opened for about 60 (mainly 59) s and aerosols were collected during these periods. Sequential opening of impactors was carried out. Two impactors were applied in the pre-conditioning phase of test, one during the SIC failure, four after SIC failure and three in the quenching period. The impactor sampling times are given in Table 1. The three BLPI samples were sampled simultaneously with AEKI impactor samples: BLPI1 simultaneously with AEKI1, BLPI2 with AEKI4, and BLPI3 with AEKI7.

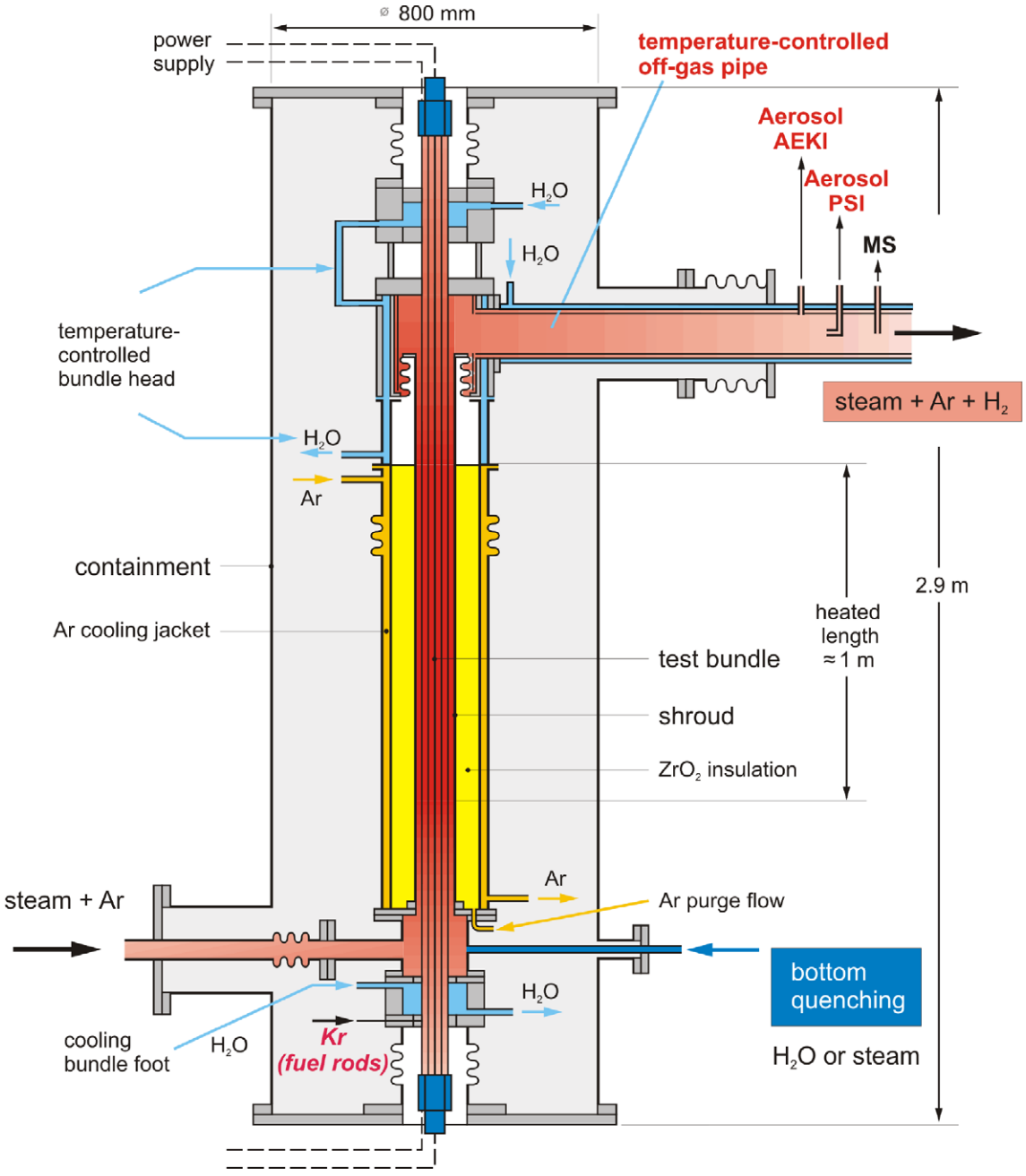

Fig. 1. Schematic of the QUENCH facility with the aerosol measurement locations.

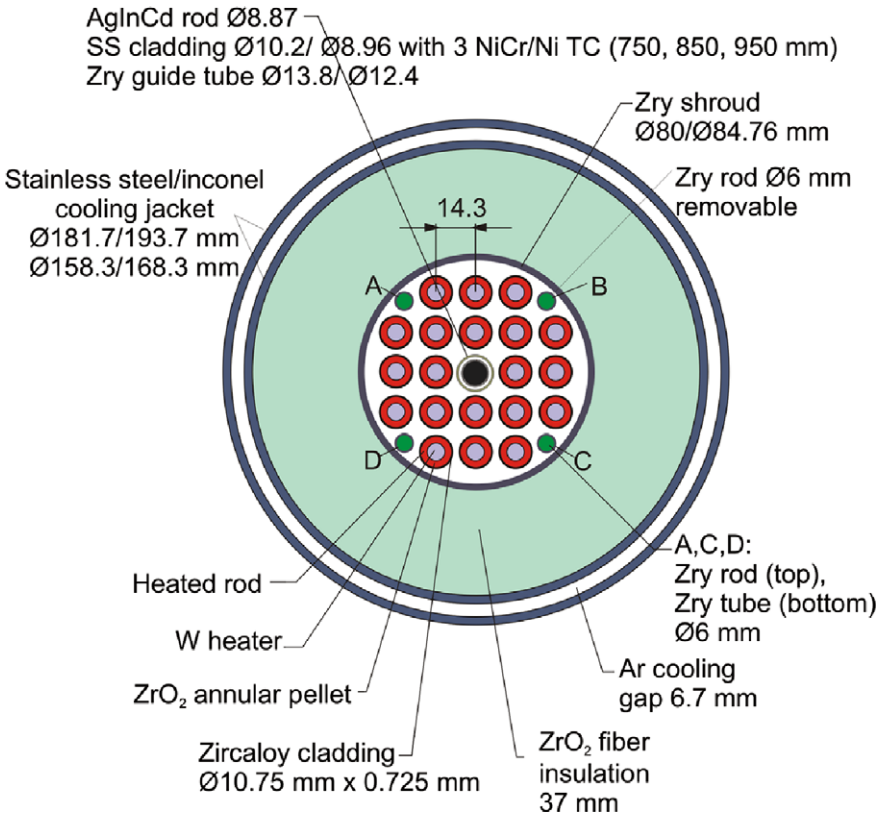

Fig. 2. Cross-section of the QUENCH-13 test bundle.

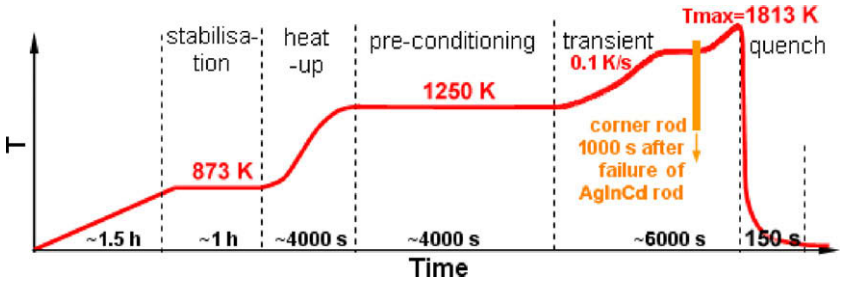

Fig. 3. Schematic of QUENCH-13 test conduct (temperature profile on hottest elevation of 950 mm).

2.3. Particle composition and morphology

After the test, samples were analyzed for particle morphology and elemental composition by scanning electron microscopy (SEM), electron microprobe (JEOL Superprobe 733) and energy-dispersive X-ray spectroscopy (EDX).

The AEKI samples were prepared for microscopy by attaching the impactor collector plates and the nickel plate on SEM sample holders by double-sided carbon tape. One quarter of the quartz fiber filters was placed on SEM holders. The SEM (Philips SEM 505) was used at 20 kV. Morphology and elemental composition with EDX (Oxford INCA) were analyzed for individual particles. Particles were analyzed generally in spot mode. In some cases where higher particle density was found, EDX analysis in area mode was applied at magnification of 3000 or 10,000.

BLPI impactor samples were prepared in a similar way: small pieces of the BLPI substrates from stages 6 (particle D_{ae} between 0.3 and 0.5 μm) and 10 (particle D_{ae} between 3.6 and 7.1 μm) were cut, and mounted on SEM sample holders using carbon tape. No other sample preparation or coating of the samples were used for elemental analyses. The SEM and EDX analyses were carried out at FZK. The electron microscope JEOL 6100 was used for the SEM images. All images were obtained with a voltage of 15 kV and a current of 2 nA. For the EDX analysis the microscope is equipped with the EUMEX Si(Li) detector S2 133 with the hydrocarbon SUTW-window. Typical energy resolution is 130 eV at 5894 eV (Mn Kα line). The EDX spot analysis with a spot diameter about 0.2 μm was used for investigation of some aerosol particles. Then the EDX integral area analyses of impactor samples were performed. The typical size of the analyzed area was 75 μm × 100 μm. The quantification of elemental concentrations was carried out with using following calibrated standards: Ag, CdS, InP, Fe, ZrO_2, SiO_2, SnO_2, Al_2O_3, TiO, W. It must be noted that elemental analyses of the impactor samples by EDX is only semi-quantitative due to the inhomogeneous sample.

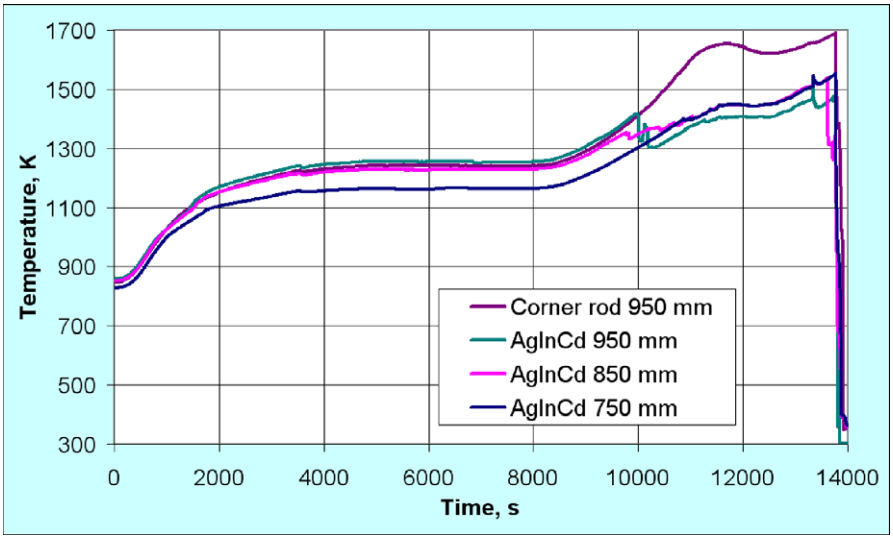

Fig. 4. Control rod and highest bundle temperatures at the QUENCH-13 test.

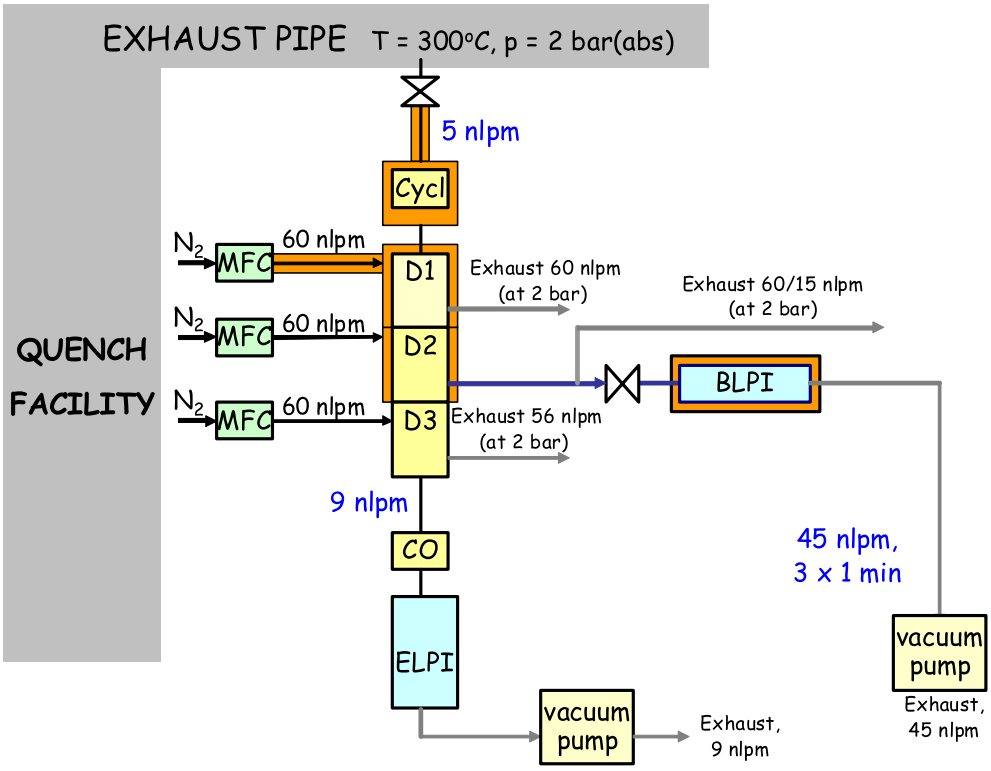

Fig. 5. Aerosol measurement set-up at QUENCH facility for the on-line measurements and BLPI.

3. Results

3.1. Particle size distribution

Aerosol particle mass size distributions were determined by ELPI and BLPI. The size distributions by both devices were similar and clearly bimodal (Fig. 8). The fine particle mode was in the particle size range D_{ae} = 0.1–2 μm. Particles larger than D_{ae} = 3 μm were also detected forming the coarse mode of the size distribution. The existence of two particle modes was confirmed by SEM analysis of the AEKI impactor samples. Two particle modes indicate that aerosol particles were formed by two mechanisms as proposed by Haste and Plumecocq [3]. However, due to the pre-cutter cyclone and the dilution units used in the measurements, the concentration of the coarse mode particles could not be determined accurately.

3.2. Particle mass concentration

The particle mass concentration of the fine particle mode in the size range D_{ae} = 0.1–2 μm as determined by BLPI after the control rod failure with two measurements at 12,118 s and 13,692 s was 450–590 mg/Nm^3 (Nm^3 = normal m^3). The average mass concentration based on 10 samples with AEKI impactors was 474 mg/m^3. The

Table 1
BLPI and AEKI impactor sampling times, duration and the maximum bundle temperature during sampling.

Sample number	Sample start time (s)	Duration (s)	Test event	T (SIC rod at 750 mm) (K)
BLPI samples				
BLPI1	7712	60	Before SIC rod failure	1240
BLPI2	12,118	60	After SIC rod failure	1630
BLPI3	13,692	75	Before bundle reflood	1690
AEKI impactors				
AEKI1	7674	58		1240
AEKI2	10,335	60		1470
AEKI3	11,097	59	After first leakage of the SIC rod and heaters	1620
AEKI4	12,070	59	After failures of the SIC rod and heaters	1630
AEKI5	13,156	59	Transient	1650
AEKI6	13,620	59	End of transient	1680
AEKI7	13,683	59	Before reflood	1690
AEKI8	13,746	59	During reflood	–
AEKI9	13,809	59	During reflood	–
AEKI10	13,871	59	During reflood	–

AEKI samples were collected during the whole test, including the quench phase (Table 1).

Continuous particle concentration measurement by ELPI shows that aerosol release started at 9400 s (Fig. 9), at the control rod $T = 1330$ K. At first, the release was very low. It increased continuously until the main aerosol release started at around 10,800 s at maximum bundle temperature $T = 1560$ K, i.e., below the stainless steel cladding melting point of ~1690 K, with two consecutive peaks in the aerosol concentration. At 11,500 s, there was a large burst of aerosol that lasted only about 100–200 s at maximum bundle temperature $T = 1650$ K. This indicates that there was a sudden release of material into the gas phase, and that the duration of this release was very short. After the large burst, aerosol concentration was relatively steady until the on-line aerosol measurement system was isolated from the QUENCH facility right before the quench phase of the test.

Fig. 8 shows that even though ELPI does not measure particle mass directly, the mass concentrations given by ELPI and BLPI are comparable. Particle mass concentration in the size range 0.1–2 μm based on the BLPI2 sample was 590 mg/Nm^3, and for the same time, mass concentration determined by ELPI was 320 mg/Nm^3. The difference in the measured concentration was presumably due, at least partly, to sampling losses in the critical orifice used with ELPI to reduce the pressure to atmospheric, to possible non-sphericity of the particles, as well as the density being different from the assumed 10 g/cm^3. In addition, it has to be noted that for larger particles, small changes in the current measured by ELPI imply large changes in mass concentration. Therefore, mass concentration of the coarse particles from ELPI should be used with some caution. Based on mass concentration derived from ELPI measurement, the total amount of aerosols in the fine particle mode in the size range 0.1–2 μm sampled at the off-gas pipe starting from time $t = 10{,}800$ s until quench at $t = 13{,}766$ s was 4.5 g. Considering losses in the critical orifice used with the ELPI, this is a lower estimate of the released fine mode particle mass.

3.3. Particle morphology and composition

During the pre-conditioning phase of the test, the AEKI1 and BLPI1 impactor samples were collected. They contained mainly Fe, Ni, Cr and Mn, i.e., impurities from stainless steel structures of the facility that were not part of the test section. A small amount of Sn originating from evaporation from Zircaloy cladding was present in sample AEKI2 corresponding to a slow increase in aerosol concentration observed starting at 9400 s. This sample was collected in the beginning of the transient.

The first aerosol peak in mass concentration was observed after 10,800 s. The AEKI3 impactor was used during this peak. The sample was rich in Cd and O, indicating that mainly Cd as was released during this first aerosol release. At aerosol sampling location at the off-gas pipe, Cd was present as an oxide.

Two types of particles were present at this time: submicrometer sized particles as determined by ELPI, and spherical particles a few micrometers in geometrical diameter, as shown in Fig. 10. The spherical particles contained mainly Cd and O, and based on their shape we suggest that they were released from the control rod as droplets. It is possible that the droplets were released as metallic Cd, and then oxidized after release from the molten surface. Due

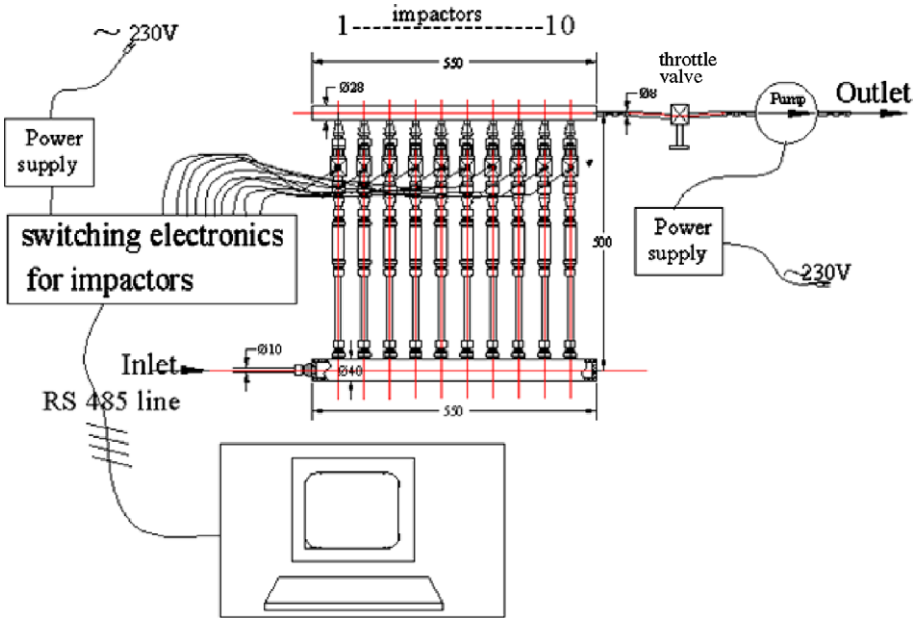

Fig. 6. Main components of the aerosol sampling system with 10 impactors supplied by AEKI.

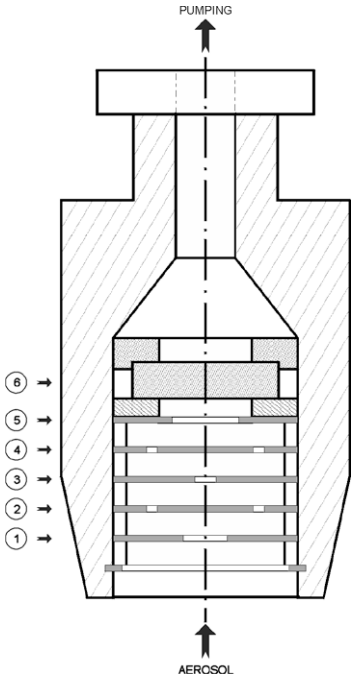

Fig. 7. Scheme of AEKI impactor sampler, 1 = 1st nozzle, 2 = 1st collector (D_{ae} > 5 μm), 3 = 2nd nozzle, 4 = 2nd collector (1 < D_{ae} < 5 μm), 5 = flow limiter, 6 = quartz fiber filter (D_{ae} < 1 μm).

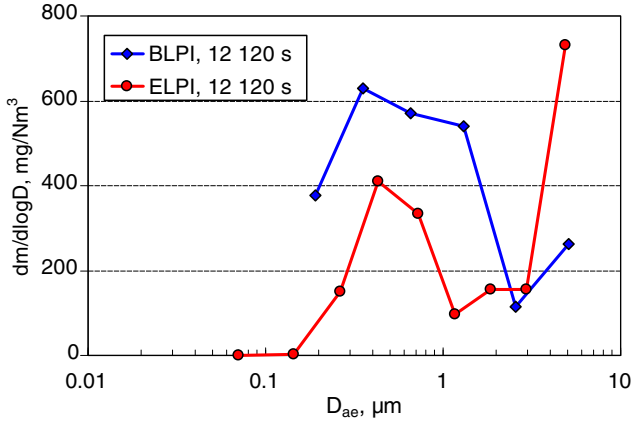

Fig. 8. Aerosol mass size distributions as determined by electrical low-pressure impactor (ELPI) and Berner low-pressure impactor (BLPI) after control rod failure at 12,118 s.

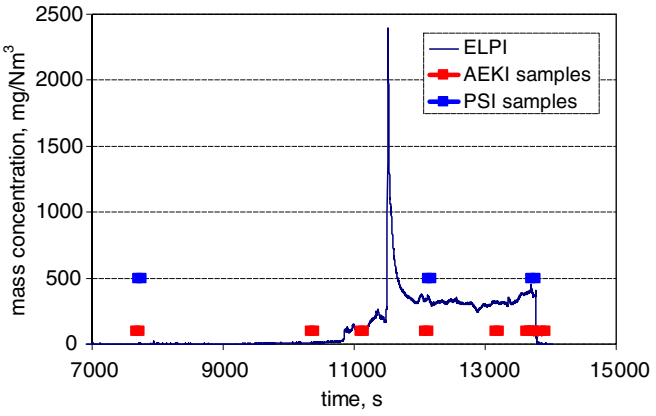

Fig. 9. Particle mass concentration in the particle size range 0.05–2 μm determined by ELPI. Blue and red squares show the sampling times with BLPI and AEKI impactors. (For interpretation of the references to colour in this figure legend, the reader is referred to the web version of this article.)

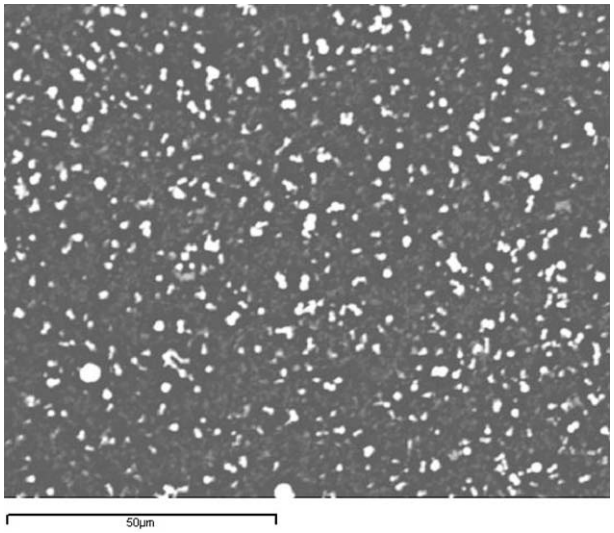

Fig. 10. Particles collected during the first aerosol peak at 11,097 s showing coarse, spherical particles.

to the high density of oxides of Cd, approximately 8 g/cm^3, the aerodynamic diameter of the approximately 2 μm spherical particles was 6 μm, clearly in the coarse particle mode as determined with ELPI and BLPI. This aerosol peak might have been caused by the existence of a small crack in the control rod cladding, through which the already vaporized Cd as well as some droplets were released.

The large aerosol burst was observed in the aerosol mass concentration at 11,500 s. AEKI4 and BLPI2 samples were collected after the large burst almost simultaneously at 12,070 s and 12,118 s, respectively. Both samples contained large amounts of Cd and In (Tables 2 and 3) as well as W from the heater rods or from the thermocouples in the facility. Elemental analysis of individual particles by EDX revealed that both Cd and In were present as oxides. A small amount of Ag was present in the fine mode particles in BLPI2 sample (impactor stage 6, D_{ae} = 0.3–0.5 μm) and the smallest particles in AEKI4. The aerosol burst was presumably caused by massive failure of the control rod.

During the steady release of aerosols after the large burst, samples AEKI5 and AEKI6 contained all the control rod materials Cd, In and Ag. The relative concentrations varied somewhat. Again, Cd and In were present as oxides, but Ag in metallic form. It has to be noted that the elemental analysis was carried out for individual particles, and therefore, the average values are not necessarily average concentrations in the samples. At this stage of the test, control rod had failed and relocated downwards in the bundle, and steady aerosol release was probably mostly due to evaporation from the molten material surface.

Two samples taken right before quench, AEKI7 at 13,683 s and BLPI3 at 13,692 s, show again all SIC control rod materials. Ag concentration as determined by BLPI increased with time, i.e., with increasing control rod temperature. This is evident by comparing the two BLPI samples, 2 and 3, that give average composition of the aerosol particles in the fine particle mode, with 2% and 7% Ag in the two samples, respectively. AEKI samples 5, 6 and 7 show large differences in the Ag concentration, presumably due to the inhomogeneous nature of the samples.

Table 2
Composition of aerosol samples collected by Berner low-pressure impactor stage 6 with D_{ae} = 0.3–0.5 μm.

Sample	End of sampling (s)	O (wt.%)	Cd (wt.%)	In (wt.%)	Ag (wt.%)	W (wt.%)	Fe (wt.%)
BLPI1	7772		–	–	–		
BLPI2	12,178	13	35	37	2	13	
BLPI3	13,767	10	30	28	7	23	2

Table 3
Average composition of individual aerosol particles analyzed in samples collected with AEKI impactors, wt.%.

Sample	Time (s)	O	Cd	In	Ag	W	Fe
AEKI3	11,156	38	62	–	–	–	–
AEKI4	12,129	28	19	38	0	15	–
AEKI5	13,215	25	9	17	4	39	0.3
AEKI6	13,679	15	0	4	58	14	3
AEKI7	13,742	30	0	6	2	0	52

Coarse, spherical particles were observed also at this time (Fig. 10). Comparing the average composition of the fine particle mode during the steady aerosol release, i.e., samples BLPI2 and BLPI3, it can be seen that concentrations of transported Cd and In were the same. Ag and W concentrations increased with time, i.e., with increasing bundle temperatures.

Quench was carried out by injecting water at the bottom of the facility at 13,766 s. The three aerosol samples collected during cooling, AEKI8-AEKI10, contained Zr, Sn and W, along with varying amounts of Cd and In. Ag and Fe were present in some distinct particles. The quantity of Cd decreased with time and Ag disappeared to the end of the sample collection. Indium decreased at first, then it increased with time. Coarse particles with irregular shapes were detected (Fig. 11), showing indication of partial melting. Particle size distributions were not determined during cooling, because on-line aerosol measurement system with the low-pressure impactor was isolated from the facility before quench.

The Ni collector that sampled particles during the whole test inside the off-gas pipe, contained: (i) Cd-rich globular particles, (ii) coarse, irregular particles enriched in Zr and O, Fig. 12, (iii) aggregates of finer particles enriched in In, and (iv) rectangular particles enriched in W, Mo, Sn and In. Because of sampling during the whole test, it is not possible to say when these different particles were collected but they give an overview of the characteristics of the coarse particles released during the test.

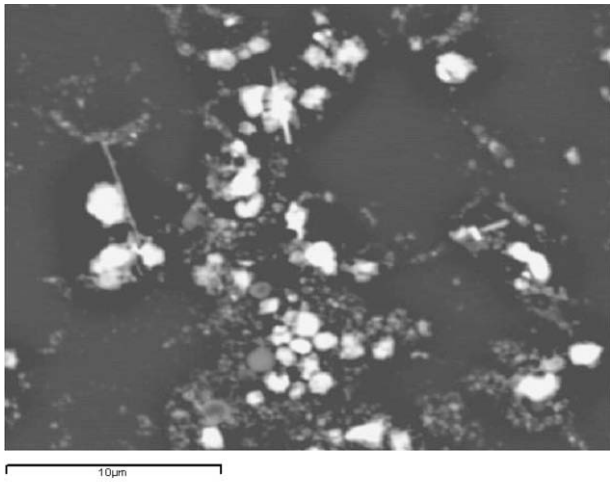

Fig. 11. SEM micrograph of particles collected during quenching, showing coarse particles.

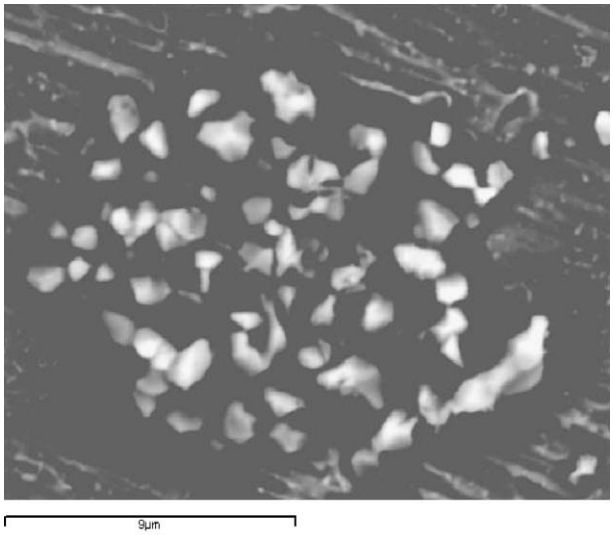

Fig. 12. SEM micrograph of particles sampled with the Ni integral collector showing coarse, irregular particles rich in Zr and O.

4. Conclusions

The QUENCH-13 test was successfully carried out to investigate effects of the control rod on degradation and reflood behavior under integral conditions, and for the first time, the release of SIC aerosols following control rod rupture was measured. Two aerosol particle modes were generated, fine mode with D_{ae} = 0.1–2 μm generated by vaporization and subsequent nucleation, condensation and coagulation, and coarse particle mode with D_{ae} > 3 μm generated by droplet release and fragmentation. These findings indicate that the commonly used modeling of aerosol formation from control rod rupture by evaporation from molten material surface would need to be refined to include aerosol generation by mechanical processes, such as droplet formation and fragment entrainment.

The aerosol generation and behavior during the test can be divided into five phases:

Transient phase: during this phase, a small but steady aerosol concentration was observed starting at 9400 s. This was presumably due to release of Sn from the Zircaloy.

First aerosol peak: first aerosol peak at 10,800 s is thought to have been caused by a small crack in the control rod cladding, and subsequent release of Cd. The particles contained mainly Cd as an oxide. Two particle modes were present, fine particle mode with particle aerodynamic diameter 0.1–2 μm, and a coarse particle mode with particles D_{ae} > 3 μm. Coarse mode particles were mainly spherical, indicating their release as droplets.

Large aerosol burst: a very large, but short aerosol burst took place at 11,500 s. The particles were mainly Cd and In, and fine mode contained small amount of Ag, indicating its release by vaporization. Cd and In were present as oxides, Ag in a metallic form. This burst was presumably due to a massive failure of the control rod.

Steady aerosol release: a steady release of aerosols followed the large burst. The particles were rich in Cd and In, and the amount of Ag increased with time. At this stage, control rod material was

relocated downwards, and aerosol was released from molten material surface.

Quench: particles released during quench phase were mainly irregular, coarse particles containing Zr, Sn and W. The particles were presumably generated by fragmentation of the Zircaloy cladding and heater elements due to thermal shocks. Information on fine mode particles during quench is not available based on this investigation.

The mass concentration of the fine aerosol mode based on BLPI measurements after the control rod failure was 450–590 mg/Nm^3. The total particle mass of the fine aerosol mode in the particle size range 0.1–2 μm during the main aerosol release period before quench during the time 10,800–13,766 s was 4.5 g, as determined in the off-gas pipe by ELPI. Mass concentration for the coarse particle mode could not be accurately determined with the experimental set-up used in this investigation. Further experimental work is needed to determine relative concentrations of the generated droplets and fragments during control rod rupture.

Acknowledgments

The authors thank Swissnuclear and Hungarian Academy of Sciences for financial support to conduct these research activities. The FZK work is sponsored by the HGF Programme NUKLEAR. The authors would like to thank Mrs. U. Stegmaier/FZK for the EDX analysis of the BLPI impactor samples. We are grateful to Dr. D. Suckow/PSI and Mr. H. Schütt/PSI for helping with the aerosol instrument preparation, and to Dr. T. Haste/PSI for initiating the work at PSI. The SARNET Network of Excellence was partly financed by the European Commission through FP6-EURATOM Contract FI6O-CT-2004-509065.

References

[1] D.A. Petti, Silver–Indium–Cadmium Control Rod Behavior and Aerosol Formation in Severe Reactor Accidents. NUREG/CR-4876, April, 1987.
[2] D.A. Petti, Nucl. Technol. 84 (1989) 128.
[3] T. Haste, W. Plumecocq, Control rod and structural material release modelling in ELSA2. in: 9th International QUENCH Workshop, FZ Karlsruhe, 13–15 October, 2003.
[4] W. Hering, P. Hofmann, Material Interactions during Severe LWR Accidents. KfK 5125, Karlsruhe, April 1994.
[5] S. Hagen, P. Hofmann, V. Noack, L. Sepold, G. Schanz, G. Schumacher, Impact of Absorber Rod Material on Bundle Degradation seen in CORA Experiments. Forschungszentrum Karlsruhe, FZKA 5680, December 1996.
[6] M. Schwarz, G. Hache, P. von der Hardt, Nucl. Eng. Des. 187 (1999) 47.
[7] B.J. Lewis, R. Dickson, F.C. Iglesias, G. Ducros, T. Kudo, J. Nucl. Mater. 380 (2008) 126–143.
[8] L. Sepold, W. Hering, G. Schanz, W. Scholtyssek, M. Steinbrück, J. Stuckert, Nucl. Eng. Des. 237 (2007) 2157–2164.
[9] J. Stuckert, L. Sepold, M. Grosse, U. Stegmaier, M. Steinbrück, J. Birchley, T. Haste, T. Lind, I. Nagy, A. Vimi, First results of the QUENCH-13 bundle experiment with a silver–indium–cadmium control rod. in: SARNET 4th Annual Review Meeting, Bled, Slovenia, 21–25 January, 2008.
[10] R. Dubourg, H. Austregesilo, C. Bals, M. Barrachin, J. Birchley, T. Haste, I. Nagy, J.-S. Lamy, T. Lind, B. Maliverney, C. Marchetto, A. Pinter, M. Steinbrück, J. Stuckert, K. Trambauer, A. Vimi, Prog. Nucl. Energy (2009), doi:10.1016/j.pnucene.2009.09.012.
[11] J. Birchley, H. Austregesilo, Ch. Bals, R. Dubourg, T. Haste, J.-S. Lamy, T. Lind, B. Maliverney, C. Marchetto, A. Pinter, M. Steinbrück, J. Stuckert, K. Trambauer, Post-test analysis of the QUENCH-13 experiment. in: Proceedings of Nuclear Energy for New Europe, Portoroz, Slovenia, September 8–11, 2008.
[12] J. Birchley, B. Jaeckel, T. Haste, M. Steinbrück, J. Stuckert, Post-test analysis of the QUENCH-13 bundle test including an Ag–In–Cd absorber rod. in: Proceedings of ICAPP 2009, Tokyo, Japan, May 10–14, 2009.
[13] L. Sepold, T. Lind, A. Pintér Csordás, U. Stegmaier, M. Steinbrück, J. Stuckert, Ann. Nucl. Energy 36 (2009) 1349–1359.
[14] Sepold, M. Heck, M. Große, T. Lind, A. Pintér Csordás, G. Schanz, U. Stegmaier, M. Steinbrück and J. Stuckert, Results of AgInCd absorber rod experiment QUENCH-13, Forschungszentrum Karlsruhe FZKA 7403, 2009.
[15] J. Keskinen, K. Pietarinen, M. Lehtimäki, J. Aerosol Sci. 23 (1992) 353–360.
[16] R.E. Hillamo, E.I. Kauppinen, Aerosol Sci. Technol. 14 (1991) 33–47.
[17] A. Pintér Csordás, L. Matus, L. Maróti, A. Czitrovszky, P. Jani, J. Aerosol Sci. 30 (1999) SI05–SI06.
[18] A. Pintér Csordás, L. Matus, Z. Hózer, A. Czitrovszky, P. Jani, J. Aerosol Sci. 31 (2000) S47–S48.
[19] A. Pintér Csordás, L. Matus, A. Czitrovszky, P. Jani, L. Maróti, Z. Hózer, P. Windberg, R. Hummel, J. Nucl. Mater. 282 (2000) 205–215.
[20] W. Koch, H. Lödding, W. Mölter, F. Munzinger, Staub Reinhalt. Luft 48 (1988).